Inter-Band GSNR Degradations and Leading Impairments in C+L Band 400G Transmission

Inter-Band GSNR Degradations and Leading Impairments in C+L Band 400G Transmission

Andrea D'Amico[(1)], Elliot London[(1)], Emanuele Virgillito[(1)], Antonio Napoli[(2)], Vittorio Curri[(1)]
[(1)]DET - Politecnico di Torino, Italy [(2)]Infinera, Germany
andrea.damico@polito.it

***Abstract*—Wideband optical transmission presents an appealing solution to network throughput and capacity requirements, improving existing network architectures with minimally invasive upgrades. This framework provides new perspectives into quality of transmission (QoT) management as a result of inter-band effects; the QoT is commonly given by the generalized signal-to-noise ratio (GSNR). In this study we address the leading impairments in multi-band nonlinear transmission in a C+L scenario from an operational point of view, supported by mathematical models and simulations. From this approach we identify that stimulated Raman scattering (SRS) is the main contributor to inter-band effects and causes the main variation in the GSNR degradation; correspondingly, we show that the inter-band nonlinear interference (NLI) can be neglected in a C+L scenario.**

***Index Terms*—wideband transmission, nonlinear interference, stimulated Raman scattering, split-step Fourier method**

I. Introduction

Network operators must aim to maximize data transport capacity in order to tackle the anticipated rapid growth of internet traffic within the next few years [1]. Developing existing optical network infrastructures has high capital expenditure (CAPEX) requirements, which has led to operators requesting that capacity is maximally exploited within existing infrastructures; in particular, operators wish to postpone the installation of new fibers, which is a capitally intensive undertaking. On a worldwide scale, standard single mode fiber (SSMF) is the most commonly deployed fiber, with the ITU-T G.652D variety presenting low losses for bandwidths exceeding 50 THz and usually with transmission restricted to the C band. One solution that vendors and operators are considering to satisfy these capacity demands is multi-band transmission, activating wavelength division multiplexing (WDM) optical line systems in spectral regions beyond the C-band [2], which is a minimally invasive step that only involves the amplification sites, the reconfigurable add-drop multiplexer nodes and requires that adequate transceiver technologies are used. The first spectral region to be exploited is the L-band, for which erbium-doped fiber amplifiers (EDFAs) and transceivers are commercially available. Implementations of C+L-band transmission have been proven to be capable of more than doubling network capacity when compared to currently-established C-band WDM transmission techniques [3], [4]. This implementation represents a highly desirable first step towards the realization of effective multi-band transmission, provided that the inter-band inter-channel (IB-IC) effects are able to be properly characterized.

Within this study, we investigate the main features of the C+L implementation from an operational point of view, considering the generalized signal-to-noise-ratio (GSNR) as the system metric. In particular, we focus our analysis on the leading contributors to the GSNR degradation in a C+L scenario, highlighting the main mutual inter-band interactions that have to be considered in order to set the system working point to a level that provides the best possible system performance. Without any loss of generality, we assume that the two most significant interaction effects between the two bands are the stimulated Raman scattering (SRS) and the Kerr effect that induces the nonlinear interference (NLI). We present the results of a split-step Fourier method (SSFM) simulation campaign in the C+L scenario, describing the IB-IC SRS and IB-IC NLI contributions, along with a comparison to an NLI model implemented in the open-source GNPy library [5], demonstrating that a fast yet accurate evaluation of the GSNR is possible, including for wideband scenarios.

II. Split-Step Fourier Method Simulations

To investigate the performance of the C+L implementation and, correspondingly, the IB-IC SRS and NLI contributions to the final GSNR degradation we perform four distinct SSFM simulations, encompassing three distinct scenarios:

- **Scenario 1**: the C and L bands are transmitted independently, with separate SSFM simulation performed for each band. In these two simulations both the intra-band SRS and the intra-band NLI have been considered.
- **Scenario 2**: the C and L bands are transmitted simultaneously, however, the IB-IC NLI is practically neglected, with the only observable inter-band interaction being the IB-IC SRS.
- **Scenario 3**: the C and L bands are transmitted simultaneously, considering both the IB-IC SRS and NLI. This simulation contains no artifacts and is the reference for the real-case C+L transmission scenario.

These simulations were performed using an accurate implementation in the MATLAB ® simulation environment [6]. For every scenario, we consider the same periodic OLS (depicted in Fig. 1(a)), consisting of 10×75 km identical spans of standard single mode fiber (SSMF) and EDFAs. Each fiber is considered to be ITU-T G.652D SSMF with a dispersion value of $16.7\,\mathrm{ps/(nm{\cdot}km)}$, nonlinear coefficient of $1.27\,(\mathrm{W{\cdot}km})^{-1}$

978-3-903176-33-1

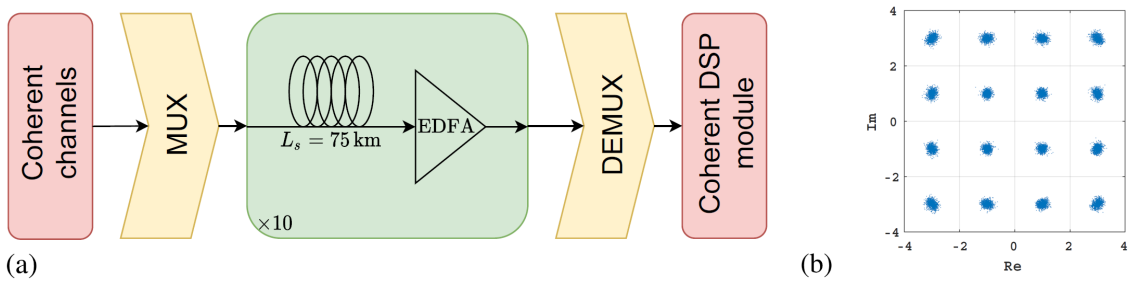

Fig. 1. (a) Schematic of the OLS under investigation. (b) A scattering diagram showing the DSP-equalized constellation of a selected CUT signal received at the OLS termination.

($A_{eff} = 80\,\mu m^2$) and a fiber loss coefficient that varies along frequency, with a mean value of 0.18 dB/km. All EDFAs operate at the same working point, completely recovering the overall fiber loss, with an output power profile that is identical to the input of each fiber span. We consider a frequency-dependent noise figure profile with an average value of 4.5 dB for evaluation of the amplified spontaneous emission (ASE) noise that is generated by the EDFAs. The transmitted signal is implemented according to the 400G standard: each channel carries a polarization multiplexed (PM) 16-QAM (quadrature amplitude modulated) signal with a symbol rate of 64 GBaud and a roll-off value of 0.15. Each band contains 64 channels equally spaced at 75 GHz frequency intervals, with a guard band of 0.5 THz in place between the bands. In total, the full C+L spectral load occupies a 10 THz bandwidth. For each band, 7 channel under tests (CUTs) have been considered and their GSNRs estimated from the error vector magnitude (EVM) on the digital signal processing (DSP)-equalized signal constellations that are received at the OLS termination. An example scattering diagram for a single CUT is shown in Fig. 1(b).

For every simulation, the launch power profile has been obtained by jointly optimizing the expected GSNR mean value and tilt, by separately varying the tilt and mean input power values for each band. This optimization is performed in order to maximize the mean GSNR value and maintain a flat profile over the entire band under investigation. The GNPy library is used to perform this optimization procedure for all scenarios. In particular, two different input power profiles have been evaluated in Scenario 1, separately optimizing the average GSNR values and tilts on each band. In Scenarios 2 and 3, the same launch power profile has been obtained by optimizing the total GSNR mean value and tilt over the full C+L scenario.

III. Results and Analysis

To properly analyze the individual inter-band effects in a C+L system, we separate the GSNR of each CUT as:

$$\mathrm{GSNR} = \left(\frac{1}{\mathrm{OSNR}} + \frac{1}{\mathrm{SNR_{NL}}} \right)^{-1}, \qquad (1)$$

where OSNR quantifies the linear contribution to the GSNR degradation, given by the total power of the ASE noise that is generated in the amplification process, whereas $\mathrm{SNR_{NL}}$ quantifies the nonlinear degradation given by the total power of the NLI noise that is generated by propagation through each fiber span.

In Fig. 2, we report the GSNR, OSNR and $\mathrm{SNR_{NL}}$ values obtained from the SSFM simulation campaign at the OLS termination for every CUT, in all investigated scenarios. As a first observation, in Fig. 2(c) it is evident that an adequate level of flatness is achieved for all scenarios under investigation, with the final GSNR profile lying within a 0.2 dB interval. Nevertheless, comparison of Fig. 2(a) and Fig. 2(b) shows that the final $\mathrm{SNR_{NL}}$ value is significantly higher with respect to the ideal value naively estimated as twice (3 dB higher than) the OSNR, [7]. This $\mathrm{SNR_{NL}}$ discrepancy may be partially explained by the optimization procedure requiring a certain level of GSNR flatness over the entire spectrum, but also arises due to an overestimation of the NLI impairment obtained using the GNPy engine. In fact, the GNPy evaluation of the NLI contribution is based on an implementation of the generalized Gaussian noise (GN) model [8]; in this framework, an average underestimation of approximately 2 dB is found in the $\mathrm{SNR_{NL}}$ prediction. A more precise description of the NLI effects can be provided considering two main corrections. First, as shown in [9], the coherent behaviour of the single-channel (SC)-NLI accumulation is taken into account by introducing an asymptotic coefficient that depends upon the chromatic dispersion, symbol rate and WDM grid. Second, the weight of cross-channel (XC)-NLI components is properly adjusted [10] to reduce the overestimation given by a similar approach in the GN model. This disaggregated methodology has been verified through an extensive simulation campaign performed in [11], leading to the following expression for the NLI noise power for a given CUT:

$$\begin{aligned} \mathrm{P_{NLI}} &= \frac{5}{6}\mathrm{C_\infty P_{SC}} + \frac{5}{6}\cdot\frac{2}{3}\mathrm{P_{XC}} \\ &= \frac{5}{6}\mathrm{C_\infty P_{SC}} + \frac{5}{6}\cdot\frac{2}{3}\mathrm{P_{XC,Intra}} + \frac{5}{6}\cdot\frac{2}{3}\mathrm{P_{XC,Inter}}\,, \end{aligned} \qquad (2)$$

where $\mathrm{C_\infty}$ is the asymptotic accumulation coefficient, $\mathrm{P_{SC}}$ and $\mathrm{P_{XC}}$ are the NLI contributions given by the SC and XC interferences, respectively. As the effect of the four-wave mixing can be neglected in the scenario under investigation, the XC-NLI component is further decomposed in the right hand side of Eq. 2; $\mathrm{P_{XC,Intra}}$ is the intra-band contribution from interfering

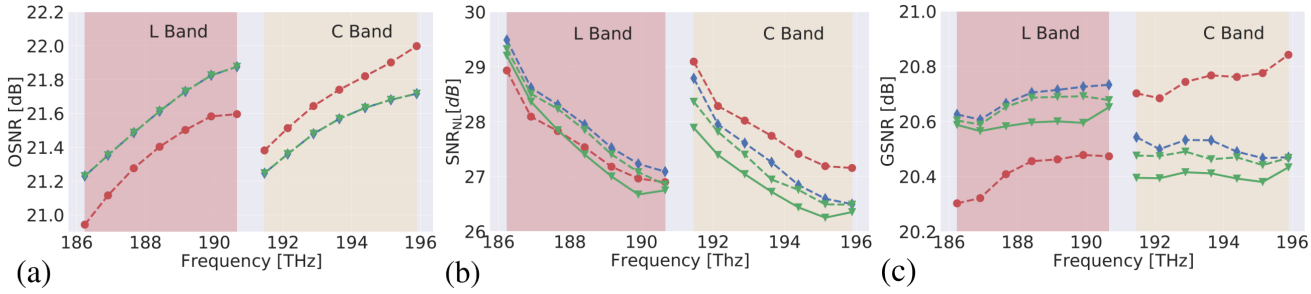

Fig. 2. (a) OSNR, (b) $\mathrm{SNR_{NL}}$ and (c) GSNR evaluated for every CUT. For all plots, the red circle, blue diamond and green triangle markers and dashed lines represent the simulation results in Scenario 1, 2 and 3, respectively. In (b) and (c) the predictions obtained using the GNPy-based model described in Section III are reported as a continuous green line.

channels within the same band of the CUT, whereas $\mathrm{P_{XC,Inter}}$ is the inter-band contribution from interfering channels within the other band, corresponding to the IB-IC NLI. In Fig. 2(b) and Fig. 2(c), we also show the results of the NLI modelling, taking these corrections into account and demonstrating an accuracy enhancement in the $\mathrm{SNR_{NL}}$ and GSNR predictions, respectively. From the simulation results for the scenarios presented in Fig. 2(c), we gain insight into the leading inter-band interactions: firstly, we observe that introducing the IB-IC SRS (passing from Scenario 1 to Scenario 2) causes the main GSNR variation for every CUT, similar to the OSNR variation that is introduced by the IB-IC SRS, visible in Fig 2(a). On the contrary, when the IB-IC NLI is introduced (passing from Scenario 2 to Scenario 3) the impact upon the GSNR variation is significantly reduced. This variation is essentially negligible for every CUT except those that are in proximity to the other band, which is still minimal. These observations allow us to conclude that the IB-IC SRS is the greatest contributor to the GSNR variation in a C+L band scenario, with the effects of the IB-IC NLI able to be neglected.

IV. Conclusion

In this work, we analyze a C+L transmission scenario in order to study the most significant aspects for QoT management. In particular, through SSFM simulations and mathematical modelling we observe that the inter-band NLI effects may be neglected, with the SRS being dominant by inducing C-to-L power transfer, within the scenario under investigation. From an operational point of view, this implies that power control in a C+L scenario must mainly consider the SRS effects as inter-band interactions that enhance the L-band and deplete the C-band. Therefore, in a power optimization scenario we stress that it is sufficient to focus upon the generation of the ASE noise and the NLI impairment that is generated by intra-band self- and cross-channel contributions.

Acknowledgments

This project has received funding from the European Union's Horizon 2020 research and innovation program under the Marie Skłodowska-Curie grant agreement 814276.

References

[1] "Cisco visual networking index: Forecast and methodology," https://www.cisco.com/c/en/us/solutions/service-provider/visual-networking-index-vni/index.html, 2018, [Online; accessed 11-March-2021].

[2] J. K. Fischer, M. Cantono, V. Curri, R.-P. Braun, N. Costa, J. Pedro, E. Pincemin, P. Doaré, C. Le Bouëtté, and A. Napoli, "Maximizing the capacity of installed optical fiber infrastructure via wideband transmission," in *2018 20th International Conference on Transparent Optical Networks (ICTON)*. IEEE, 2018, pp. 1–4.

[3] V. Lopez, B. Zhu, D. Moniz, N. Costa, J. Pedro, X. Xu, A. Kumpera, L. Dardis, J. Rahn, and S. Sanders, "Optimized design and challenges for c&l band optical line systems," *Journal of Lightwave Technology*, vol. 38, no. 5, pp. 1080–1091, 2020.

[4] J.-X. Cai, H. Batshon, M. V. Mazurczyk, O. V. Sinkin, D. Wang, M. Paskov, W. Patterson, C. R. Davidson, P. Corbett, G. Wolter *et al.*, "70.4 tb/s capacity over 7,600 km in c+ l band using coded modulation with hybrid constellation shaping and nonlinearity compensation," in *Optical Fiber Communication Conference*. Optical Society of America, 2017, pp. Th5B–2.

[5] A. Ferrari, M. Filer, K. Balasubramanian, Y. Yin, E. Le Rouzic, J. Kundrat, G. Grammel, G. Galimberti, and V. Curri, "Gnpy: an open source application for physical layer aware open optical networks," *Journal of Optical Communications and Networking*, vol. 12, no. 6, pp. C31–C40, 2020.

[6] D. Pilori, M. Cantono, A. Carena, and V. Curri, "FFSS: The fast fiber simulator software," in *2017 19th International Conference on Transparent Optical Networks (ICTON)*, 2017, pp. 1–4.

[7] R. Pastorelli, S. Piciaccia, G. Galimberti, E. Self, M. Brunella, G. Calabretta, F. Forghieri, D. Siracusa, A. Zanardi, E. Salvadori *et al.*, "Optical control plane based on an analytical model of non-linear transmission effects in a self-optimized network," in *39th European Conference and Exhibition on Optical Communication (ECOC 2013)*. IET, 2013, pp. 1–3.

[8] M. Cantono, D. Pilori, A. Ferrari, C. Catanese, J. Thouras, J.-L. Augé, and V. Curri, "On the interplay of nonlinear interference generation with stimulated raman scattering for qot estimation," *Journal of Lightwave Technology*, vol. 36, no. 15, pp. 3131–3141, 2018.

[9] A. D'Amico, E. London, E. Virgillito, A. Napoli, and V. Curri, "Quality of transmission estimation for planning of disaggregated optical networks," in *2020 International Conference on Optical Network Design and Modeling (ONDM)*. IEEE, 2020, pp. 1–3.

[10] E. Virgillito, A. D'Amico, A. Ferrari, and V. Curri, "Observing and modeling wideband generation of non-linear interference," in *2019 21st International Conference on Transparent Optical Networks (ICTON)*. IEEE, 2019, pp. 1–4.

[11] E. London, E. Virgillito, A. D'Amico, A. Napoli, and V. Curri, "Simulative assessment of non-linear interference generation within disaggregated optical line systems," *OSA Continuum*, vol. 3, no. 12, pp. 3378–3389, 2020.